Food and Chemical Toxicology 131 (2019) 110533

Contents lists available at ScienceDirect

Food and Chemical Toxicology

journal homepage: www.elsevier.com/locate/foodchemtox

2′,4′-Dihydroxy-6′-methoxy-3′,5′-dimethylchalcone induced apoptosis and G1 cell cycle arrest through PI3K/AKT pathway in BEL-7402/5-FU cells

Xiang Ji[a,1], Xing Wei[a,1], Jie Qian[b], Xuejun Mo[a], Guoyin Kai[c], Faliang An[a,**], Yanhua Lu[a,*]

[a] State Key Laboratory of Bioreactor Engineering, East China University of Science and Technology, 130 Meilong Road, Shanghai, 200237, People's Republic of China
[b] School of Life Sciences and Technology, Tongji University, Shanghai, 200092, People's Republic of China
[c] College of Pharmacy, Zhejiang Chinese Medical University, Hangzhou, 310053, People's Republic of China

ARTICLE INFO

Keywords:
2′,4′-Dihydroxy-6′-methoxy-3′,5′-dimethylchalcone (DMC)
Apoptosis
Cell cycle arrest
AKT
Hepatocellular carcinoma

ABSTRACT

Hepatocellular carcinoma is the fifth most common and the third most lethal cancer worldwide. In recent years, natural flavonoids have drawn great attention as repository for the exploitation of novel antineoplastic agents. 2′,4′-Dihydroxy-6′-methoxy-3′,5′-dimethylchalcone (DMC), a functional chalcone isolated from the buds of *Cleistocalyx operculatus*, has been reported to exert potent cytotoxicity against multi-drug resistant BEL-7402/5-FU cells. In this study, the precise mechanisms of DMC-mediated growth inhibition in BEL-7402/5-FU cells were further investigated. DMC was found to trigger apoptosis predominantly via the mitochondria-dependent pathway and the enhancement of reactive oxygen species (ROS) generation. Meanwhile, DMC induced G1 cell cycle arrest through downregulation of cyclin D1 and CDK4. Furthermore, DMC increased p53 level and inhibited NF-κB nuclear-localization via suppression of PI3K/AKT signaling axis, which might be the underlying mechanism of DMC-induced apoptosis and cell cycle arrest in BEL-7402/5-FU cells. Collectively, the study elucidated the mechanisms by which DMC may inhibit the growth of BEL-7402/5-FU cells and suggested the possibility that DMC might be a promising candidate therapeutic agent for hepatoma treatment in the future.

1. Introduction

Hepatocellular carcinoma (HCC), a sort of high-incidence digestive system cancer, is recognized as the second most lethal malignancy in men (Ferlay et al., 2015). HCC is generally insusceptible to chemotherapy due to the intrinsic resistance or the acquired resistance that forms over the duration of treatment (Zhou et al., 2017a,b), which remains a principal impediment in chemotherapy treatment for HCC. Hence, there have been urgent demands for the exploitation of natural products as substitutes or adjuvants for cancer treatment.

Apoptosis, also known as programmed cell death, plays pivotal roles in diverse physiological and pathological processes (Hou et al., 2016). Evasion of apoptosis will contribute to oncogenesis and endow tumor cells with resistance against chemotherapy (He et al., 2008). Induction of apoptosis in tumor cells is an effective therapeutic strategy of antineoplastic agents. Moreover, cell cycle is a string of cellular events responsible for DNA duplication and cell proliferation, which consists of four sequential phases (G0/G1, S, G2 and M). The cell cycle progression is systematically propelled via the modulation of a series of cyclins (CCNs), cyclin-dependent kinases (CDKs) and cyclin-dependent kinase inhibitors (CKIs) (Asghar et al., 2015). The aberrant acceleration of cell cycle activities causes uncontrollable cell multiplication and loss of differentiation, which is taken as a hallmark of cancer (Wang et al., 2018a,b). It has been found that over 90% of human cancers are related to the speeding up of G1 phase on account of variations in CCNs, CDKs and CKIs (Bonelli et al., 2014). Consequently, the use of agents targeting cell cycle regulators and inducing blockage at certain phase comes to be an efficacious strategy for tumor regression.

Phosphatidylinositol 3-kinase/protein kinase B (PI3K/AKT) pathway was documented to be frequently activated in cancer cells (Hou et al., 2016), impacting a considerable array of intracellular events responsible for cell survival and apoptosis avoidance (Lewis-Wambi and Jordan, 2009). In relation to these events, nuclear factor-kappa B (NF-κB) and p53 are the most studied downstream effectors.

* Corresponding author. State Key Laboratory of Bioreactor Engineering East China University of Science and Technology, Box 283#, 130 Meilong Road, Shanghai, 200237, People's Republic of China.
** Corresponding author. State Key Laboratory of Bioreactor Engineering, East China University of Science and Technology, Box 283#, 130 Meilong Road, Shanghai, 200237, People's Republic of China.
E-mail addresses: flan2016@ecust.edu.cn (F. An), luyanhua@ecust.edu.cn (Y. Lu).
[1] Contributed equally to this work.

https://doi.org/10.1016/j.fct.2019.05.041
Received 25 January 2019; Received in revised form 7 May 2019; Accepted 27 May 2019
Available online 28 May 2019

NF-κB is a pro-survival transcription factor primarily activated through AKT direct phosphorylation on inhibitor of NF-κB (IκB) kinase (IKK). The main function of NF-κB involves coordinating the expression of a battery of anti-apoptotic genes such as Bcl-2 and Bcl-xL, which results in the suppression of apoptosis machinery (Saha et al., 2015). As another broadly investigated tumor suppressor regulated by AKT, p53 has wide-spectrum functions including maintaining genomic integrity, regulating cell cycle progression and inducing apoptosis (Vousden and Prives, 2009). Murine double minute 2 (Mdm2), a cellular phosphoprotein activated by AKT, functions as an inhibitor of p53 by forming a complex with p53 and mediating p53 degradation via its E3 ubiquitin ligase activity (Momand et al., 1998). Suppression of p53 or excessive activation of Mdm2 was found to be correlated with cancer onset (Nag et al., 2014). It is therefore reasonable for us to pinpoint AKT, p53 and NF-κB as potential targets of apoptosis induction in BEL-7402/5-FU cells.

Natural flavonoids have received considerable attention as candidates for novel antineoplastic agent development in recent years (Zhang et al., 2018). Current studies have suggested that dietary intake of flavonoids is correlated with a lower risk of carcinogenesis (Jeong et al., 2009). DMC, a novel naturally-formed chalcone extracted from the buds of *Cleistocalyx operculatus* (Roxb.) Merr. et Perry (Myrtaceae) that was taken as herbal tea as well as traditional Chinese medicine, has been reported to possess significant antitumor activities against SMMC-7721 cells and K562 cells (Ye et al., 2004, 2005). Previous studies of our group have indicated that DMC exhibited growth-inhibiting and apoptosis-inducing effects in BEL-7402/5-FU cells (Huang et al., 2011, 2012). However, the precise signal transduction mechanisms remain unclear. Thus, the present study aims to illustrate the mechanisms of DMC-mediated growth inhibition in BEL-7402/5-FU cells in terms of its modulation on apoptosis and cell cycle. The molecular events underlying DMC-induced apoptosis and cell cycle arrest were also explored, which were correlated with PI3K/AKT pathway-dependent regulation of Mdm2/p53 and IKK/NF-κB.

2. Materials and methods

2.1. Cell culture and reagents

The HCC multi-drug resistant cell line BEL-7402/5-FU and its parental cell line BEL-7402 were purchased from KeyGen Biotech (Nanjing, China). BEL-7402 cells were cultured in RPMI-1640 medium supplemented with 10% fetal bovine serum (Gibco, NY, USA) at 37 °C with 5% CO_2, and BEL-7402/5-FU cells were cultured with additional 20 μg/mL 5-fluorouracil (5-FU). The BEL-7402/5-FU cells were cultured in RPMI-1640 medium without 5-FU for 2 weeks before all experiments.

DMC was isolated from the buds of *Cleistocalyx operculatus*, and its chemical structure is depicted in Fig. 1. The purity of DMC was greater than 98% as determined by HPLC.

The primary antibodies against p-PI3K p85 (Tyr-458), NF-κB p65 and p53 were purchased from Cell Signaling Technology (MA, USA). Antibodies against p-Mdm2 (Ser-166) and p-IKK α/β (Ser-180/Ser-181) were purchased from Bioworld (MN, USA). A mouse antibody against β-actin was purchased from ProteinTech (IL, USA). Antibodies against Bcl-2, Bcl-xL, Bax, Bad, cytochrome c (Cyt-c), VDAC1, PARP/cleaved PARP, cleaved caspase-3, cleaved caspase-9, survivin, clusterin β, XIAP, Fas L, DR5, procaspase-8, cleaved caspase-8, cleaved Bid, p-GSK3β (Ser-9), GSK3β, cyclin D1, CDK4, p21, PI3K, p-AKT (Ser-473), AKT, Mdm2, IKK α/β, Histone H3 and Lamin B were purchased from Wanlei (Shenyang, China). FITC-labeled Goat Anti-Rabbit IgG (H + L) was purchased from Biotech Well (Shanghai, China).

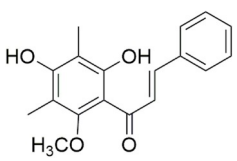

Fig. 1. The chemical structure of DMC.

2.2. Cell viability assay

The cytotoxic effects of DMC and 5-FU on BEL-7402 and BEL-7402/5-FU cells were determined by cell viability assay. Exponentially proliferating BEL-7402 and BEL-7402/5-FU cells were seeded into 96-well plates at a density of 7×10^3 cells/well and cultured overnight. After cells were exposed to various concentrations of DMC or 5-FU for 48 h, the original medium was replaced with medium containing 0.5 mg/mL 3-(4,5-dimethylthiazol-2-yl)-2,5-diphenyltetrazolium bromide (MTT). After 4 h of incubation, the medium was removed, and 150 μL of DMSO was added to each well to dissolve the formazan. The absorbance of the products at 570 and 630 nm was detected by the microplate reader (SpectraMax i3; Molecular Devices, CA, USA).

2.3. Measurement of ROS level

The effect of DMC on intracellular ROS level was examined by ROS Detection Kit (KeyGen, Nanjing, China) via 2′,7′-dichlorofluorescein diacetate (DCFH-DA) assay. After treatment with DMC for 24 h, cells were collected and incubated with DCFH-DA at 37 °C for 20 min and then washed with PBS. The fluorescence value was detected at 488 nm and 525 nm by microplate reader (SpectraMax i3; Molecular Devices, CA, USA). The intracellular ROS content was normalized to the total protein level of each sample.

2.4. Determination of apoptosis by annexin V-FITC/PI double staining

The effects of DMC and 5-FU on apoptosis in BEL-7402/5-FU cells were determined by Annexin V-FITC Apoptosis Detection Kit (Beyotime, Haimen, China). After treatment with indicated concentrations of DMC or 5-FU for 48 h, cells were collected and washed with PBS. Then 195 μL of Annexin V-FITC binding buffer was added to each sample, followed by 5 μL of Annexin V-FITC staining solution and 10 μL of propidium iodide. Cells were incubated with the dye for 20 min at room temperature (25 °C) and subsequently determined by flow cytometry analysis (FACSAria; BD Biosciences, CA, USA). Results were analyzed by FlowJo 10.0.7 (Flexera Software, IL, USA).

2.5. Flow cytometry analysis for cell cycle

The effect of DMC on cell cycle progression was measured by the Cell Cycle and Apoptosis Analysis Kit (Wanlei, Shenyang, China). After incubation with various concentrations of DMC for 24 h, cells were harvested, resuspended and incubated in 70% cold ethanol overnight. Then cells were incubated with RNase at 37 °C for 30 min, followed by incubation with PI in the dark for 30 min. Cell cycle distribution was assessed by the flow cytometer (FACSAria; BD Biosciences, CA, USA) at 488 nm. The results were analyzed by Modfit (Verity Software House, ME, USA).

2.6. Western blot assay

The BEL-7402/5-FU cells were seeded into 6-well plates and cultured overnight. After treatment with DMC, total protein was obtained by cell lysis buffer for Western and IP (Biotech Well, Shanghai, China). The nuclear, mitochondrial and cytoplasmic fractions were prepared using Nuclear and Cytoplasmic Protein Extraction Kit (KeyGen, Nanjing, China) and Cell Mitochondria Isolation Kit (Beyotime, Haimen, China), respectively. The protein contents were assessed by BCA assay. Equal quality of protein (20 μg/lane) from each sample was separated in SDS-polyacrylamide gels of different concentrations and

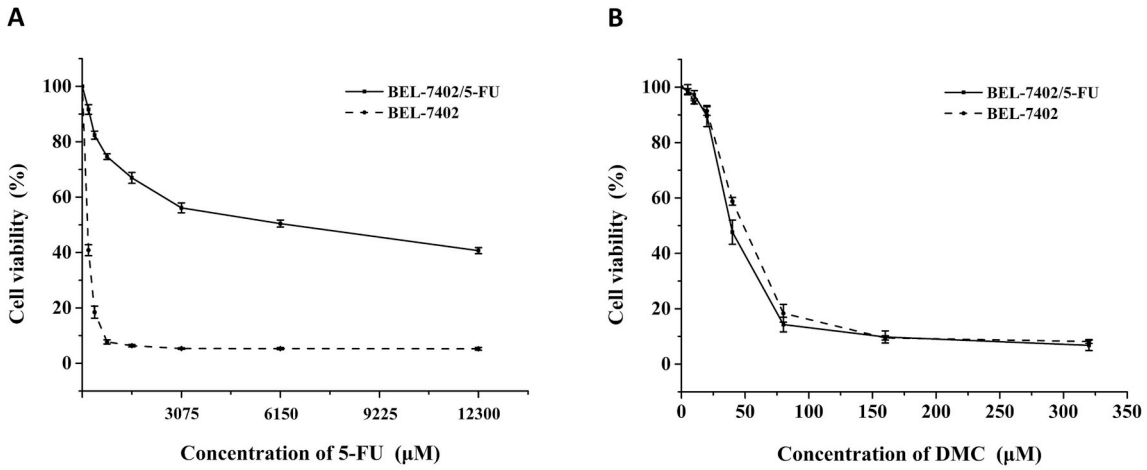

Fig. 2. Cytotoxic effects of 5-FU and DMC on BEL-7402 and BEL-7402/5-FU cells. After BEL-7402 and BEL-7402/5-FU cells were treated with different concentrations of 5-FU or DMC for 48 h, cell viability was assessed by MTT assay. Data are presented as mean ± SD. Results are representative of three independent experiments.

successively electrotransferred onto the polyvinylidene fluoride membrane (Millipore, MA, USA). The membranes were then blocked with 5% BSA in TBST for 2 h prior to incubation with corresponding primary antibodies at 4 °C overnight. Subsequently, membranes were probed with HRP-conjugated secondary antibodies. The bands were visualized by the BeyoECL Moon reagent (Beyotime, Haimen, China) via the Bio-electrophoresis Image Analysis System (FR-1800; Furi, Shanghai, China).

2.7. Immunocytochemistry

The abacterial coverslips (14 mm) were placed into the 6-well plates, and cells were evenly seeded onto each at a density of 1×10^4 cells/mL. After treatment with DMC, cells were washed twice with PBS and then fixed with 4% paraformaldehyde for 20 min and perforated with 0.3% Triton X-100 for 30 min. Afterwards, cells were blocked with 5% BSA for 1 h and incubated with NF-κB antibody at 4 °C overnight, followed by being probed with FITC-labeled goat anti-rabbit IgG (H + L) (Biotech Well, Shanghai, China) in the dark for 2 h. After samples were washed 3 times with PBS, DAPI Fluoromount-G™ (Yeasen, Shanghai, China) was added onto the middle of each coverslip. The coverslips were inverted onto the glass slides before observations. Samples were then photographed by the fluorescence microscope (Eclipse Ti; Nikon, Japan).

2.8. Transient transfection with AKT small interfering RNA (siRNA)

The AKT-siRNA (sense: 5′-GCACUUUCGGCAAGGUGAUTT-3′; anti sense: 5′-AUCACCUUGCCGAAAGUGCTT-3′) and the negative control siRNA (sense: 5′-UUCUCCGAACGUGUCACGUTT-3′; anti sense: 5′-ACG UGACACGUUCGGAGAATT-3′) were designed and synthesized by GenePharma (Shanghai, China). For AKT knock-down, exponentially proliferating BEL-7402/5-FU cells were seeded into 6-well plates at a density of 4×10^4 cells/well and the confluence was maintained at approximately 60%. After 100 pmol negative control siRNA or AKT-siRNA in 125 μL of RPMI-1640 and 5 μL of siRNA-Mate transfection reagent in 125 μL of RPMI-1640 were let stand separately for 5 min, the medium containing siRNA and the medium containing transfection reagent were mixed up and stood for 20 min. The original medium in the plates was then replaced by 2 mL of antibiotic/serum-free RPMI-1640 medium per well. The mixture was added to each well and incubated for 5 h. Afterwards, the transfection mixture was discarded, and cells were treated with medium with or without 10 μM DMC for 48 h. Cells were harvested and the whole-cell lysates were subjected to western blotting.

2.9. Statistical analysis

Results are presented as the mean ± standard deviation (SD) from three replicates for each sample. Statistical analyses were performed using SPSS 19.0 (SPSS Inc., IL, USA). Differences between groups were determined by ANOVA analysis. A value of $P < 0.05$ was considered statistically significant.

3. Results

3.1. Cytotoxic effects of DMC and 5-FU on BEL-7402 and BEL-7402/5-FU cells

To verify the chemoresistance of the resistant cell line and the effective cytotoxicity of DMC, the effects of DMC and 5-FU on the viability of BEL-7402 and BEL-7402/5-FU cells were evaluated through MTT assay. As Fig. 2 shows, both 5-FU (Fig. 2A) and DMC (Fig. 2B) concentration-dependently inhibited the growth of BEL-7402 and BEL-7402/5-FU cells. The IC_{50} values of DMC in BEL-7402 and BEL-7402/5-FU cells were 47.24 ± 0.46 μM and 44.23 ± 3.50 μM, respectively. The IC_{50} values of 5-FU in BEL-7402 and BEL-7402/5-FU cells were 69.96 ± 10.69 μM and 5662.82 ± 245.77 μM, respectively. The resistance index of BEL-7402/5-FU cells against 5-FU was 80.95, which indicated that the two cell lines showed similar susceptibility to DMC but BEL-7402/5-FU cells were resistant to 5-FU. The results were in accordance with those of the previous work done by our group (Huang et al., 2011).

3.2. DMC induced apoptosis in BEL-7402/5-FU cells

To unveil the detailed mechanisms of the inhibitory effects mediated by DMC and 5-FU in BEL-7402/5-FU cells, the effects of the two agents on the apoptosis rate in the resistant cells were assessed by Annexin V-FITC/PI double staining assay. As shown in Fig. 3, compared with 5-FU, DMC induced more prominent apoptosis at a lower dose, expounding that the growth inhibition in BEL-7402/5-FU cells mediated by DMC might be due to their susceptibility to DMC-mediated apoptosis.

3.3. DMC augmented the intracellular ROS level

Induction of ROS is one of the strategies of anti-tumor agents for

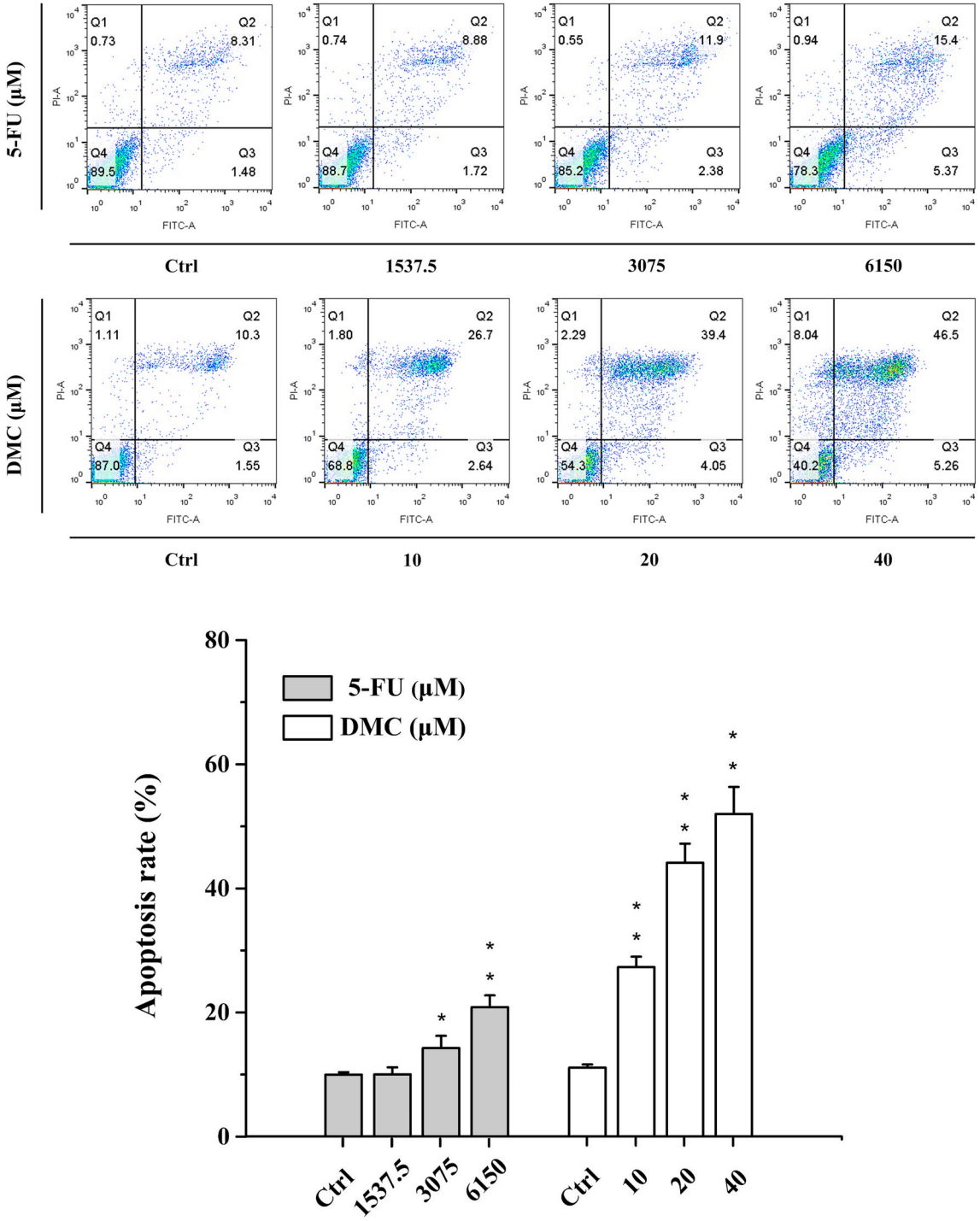

Fig. 3. Effects of 5-FU and DMC on apoptosis rate in BEL-7402/5-FU cells. BEL-7402/5-FU cells were exposed to indicated concentrations of DMC or 5-FU for 48 h. Double staining with FITC-conjugated Annexin V and PI assay was undertaken to analyze apoptosis. Data are presented as mean ± SD. Results are representative of three independent experiments. (*) $P < 0.05$ and (**) $P < 0.01$, compared with the control.

inhibiting tumor cell proliferation. To investigate whether DMC induced apoptosis by promoting the generation of intracellular ROS, ROS content in BEL-7024/5-FU cells treated with DMC was assessed. As Fig. 4 shows, compared with the control group, intracellular ROS level of DMC-treated group was elevated in a DMC dose-dependent manner, suggesting that DMC could trigger apoptosis in BEL-7024/5-FU cells by enhancing the generation of ROS.

3.4. Effects of DMC on intrinsic and extrinsic apoptosis pathways

Apoptosis is generally categorized into intrinsic pathway and extrinsic pathway. To determine whether the intrinsic or extrinsic pathway was involved in DMC-induced apoptosis, the effects of DMC on key proteins of the two pathways were investigated. As shown in Fig. 5A, the expression of pro-apoptotic Bax and Bad was upregulated,

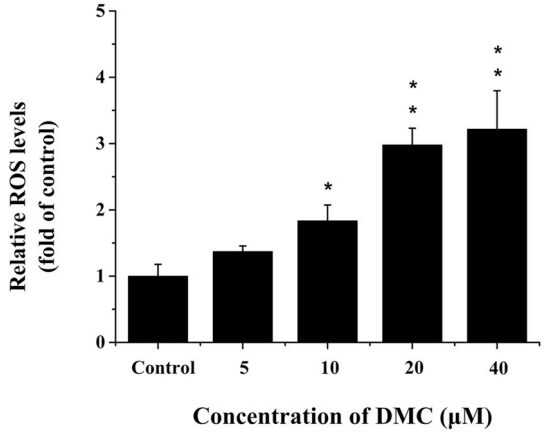

Fig. 4. DMC elevated intracellular ROS level in BEL-7402/5-FU cells. Cells were treated with DMC for 24 h. The ROS level was detected according to the manufacturer's instructions. Results were normalized to the total protein level of each sample. Data are presented as mean ± SD. Results are representative of three independent experiments. (*) $P < 0.05$ and (**) $P < 0.01$, compared with the control.

while the expression of anti-apoptotic Bcl-2 and Bcl-xL was decreased. Moreover, as presented in Fig. 5B, DMC reduced the mitochondrial cytochrome c and increased its content in cytoplasm. Meanwhile, levels of cleaved caspase-3 and cleaved caspase-9 were found to increase significantly. As a consequence of caspase-3 activation, an increased level of PARP cleavage was also observed. In addition, as Fig. 5C shows, DMC attenuated the expression of clusterin β and XIAP but did not significantly alter the level of survivin. Furthermore, DMC showed no remarkable effect on key proteins of the extrinsic apoptosis pathway (Fig. 6). These results collectively suggested that DMC induced apoptosis in BEL-7402/5-FU cells mainly through the mitochondrial apoptosis pathway.

3.5. DMC induced cycle arrest at G1 phase

To clarify whether the DMC-induced growth inhibitory effect was related to cell cycle perturbation, the cell cycle distribution of BEL-7402/5-FU cells after DMC treatment was determined. As shown in Fig. 7, the proportion of G1 phase cells was increased dramatically after DMC treatment, which indicated that DMC exerted cytotoxicity against BEL-7402/5-FU cells partly owing to the blockage at the G1 phase of cell cycle.

3.6. DMC regulated cell cycle G1-related proteins

Cell cycle progression is regulated by phase-specific checkpoint proteins. To further elucidate the molecular mechanism of DMC-induced G1 cell cycle arrest in BEL-7402/5-FU cells, the G1 phase related proteins were evaluated through western blotting. As shown in Fig. 8, DMC concentration-dependently attenuated the levels of p-GSK3β, cyclin D1 and CDK4. GSK3β and p21, the negative regulators of cyclin D1 and CDK4, were significantly elevated after DMC treatment. These results demonstrated that DMC induced the arrest of cell cycle at G1 phase through the downregulation of p-GSK3β, cyclin D1 and CDK4 and the upregulation of GSK3β and p21.

3.7. DMC regulated the key proteins of PI3K/AKT pathway

PI3K/AKT pathway plays a pivotal role in the progression of carcinogenesis and chemoresistance. To ascertain whether DMC overcomes chemoresistance through regulating PI3K/AKT pathway, the effects of DMC on the key targets of PI3K/AKT pathway were assessed by western blotting. As displayed in Fig. 9A, DMC dose-dependently suppressed the phosphorylation of PI3K and AKT as well as their downstream targets Mdm2 and IKK. After incubation with DMC for 2–8 h, the accumulation of p53 was remarkably augmented in both nucleus and in cytoplasm (Fig. 9B), and NF-κB was decreased in nucleus and increased in cytoplasm (Fig. 9C). The decrease in nuclear translocation of NF-κB was subsequently verified by immunofluorescence. As shown in Fig. 9D, NF-κB characterized by the green fluorescence gathered in the nucleus in the control group, however, as DMC treatment time prolonged, the green fluorescence started to increase in the cytosol, which was consistent with the western blotting results. These results demonstrated that DMC deactivated PI3K/AKT pathway and thus negatively modulated the activity of the downstream factors Mdm2 and IKK, which ultimately contributed to the accumulation of p53 and nuclear translocation inhibition of NF-κB.

After incubation with indicated concentrations of DMC for 24 h, the whole-cell lysates were prepared, and the expression levels of p-PI3K, PI3K, p-AKT, AKT, p-Mdm2, Mdm2, p-IKK and IKK were determined by western blotting (A). After incubation with 10 μM DMC for 2, 4 and 8 h, the nuclear and cytoplasmic fractions were prepared, and the expression levels of p53 (B) and NF-κB (C) were determined by western blotting. β-actin served as the loading control for the cytoplasmic protein. Histone H3 or Lamin B served as the loading control for the nuclear protein. The translocation of NF-κB was verified by immunofluorescence (D). Data are presented as mean ± SD. Results are representative of three independent experiments. (*) $P < 0.05$ and (**) $P < 0.01$, compared with the control.

To further confirm whether the regulatory effects of DMC on mitochondrial apoptosis proteins were mediated by AKT, the knockdown of AKT was performed in BEL-7402/5-FU cells through transient transfection of AKT-siRNA. As shown in Fig. 10, in the non-targeting control group, DMC treatment increased the levels of Bax and Bad and decreased Bcl-2 expression. Similarly, AKT-knockdown resulted in the elevation of Bax and Bad expression and the decline of Bcl-2. Moreover, in AKT-siRNA group, the AKT-knockdown abrogated DMC-induced alterations in Bcl-2 family proteins to some extent, implying that DMC affected the mitochondrial apoptosis pathway at least partially through the PI3K/AKT signaling axis.

4. Discussion

Hepatocellular carcinoma (HCC) is the fifth most common and the third most lethal cancer worldwide (Tao et al., 2018). Currently, 5-FU-based regimens are taken as one of the most used therapies for HCC treatment. However, the overall response of HCC to chemotherapeutics is still far from satisfactory (Gu et al., 2012; Zhang et al., 2008), instigating the revision of the conventional cure strategy and the demand for the exploitation of natural remedies as candidate anticancer agents. DMC, a naturally-formed chalcone, has been reported to inhibit proliferation and overcome multi-drug resistance of BEL-7402/5-FU cells (Wei et al., 2018; Huang et al., 2011), while the concrete mechanisms of the growth inhibitory effect remain unclear. This study focused on revealing the molecular mechanisms underlying the cytotoxic effect of DMC in BEL-7402/5-FU cells in terms of its regulation on apoptosis and cell cycle progression.

In the present study, we verified that the resistance index of BEL-7402/5-FU against 5-FU was 80.95. The IC_{50} values of DMC in BEL-7402 and BEL-7402/5-FU cells were 47.24 ± 0.46 μM and 44.23 ± 3.50 μM, respectively, indicating that BEL-7402/5-FU cells exhibited greater sensitivity to DMC treatment. Flow cytometry results showed that low-dose DMC induced more prominent apoptosis in BEL-7402/5-FU cells than 5-FU did, which might explain the growth

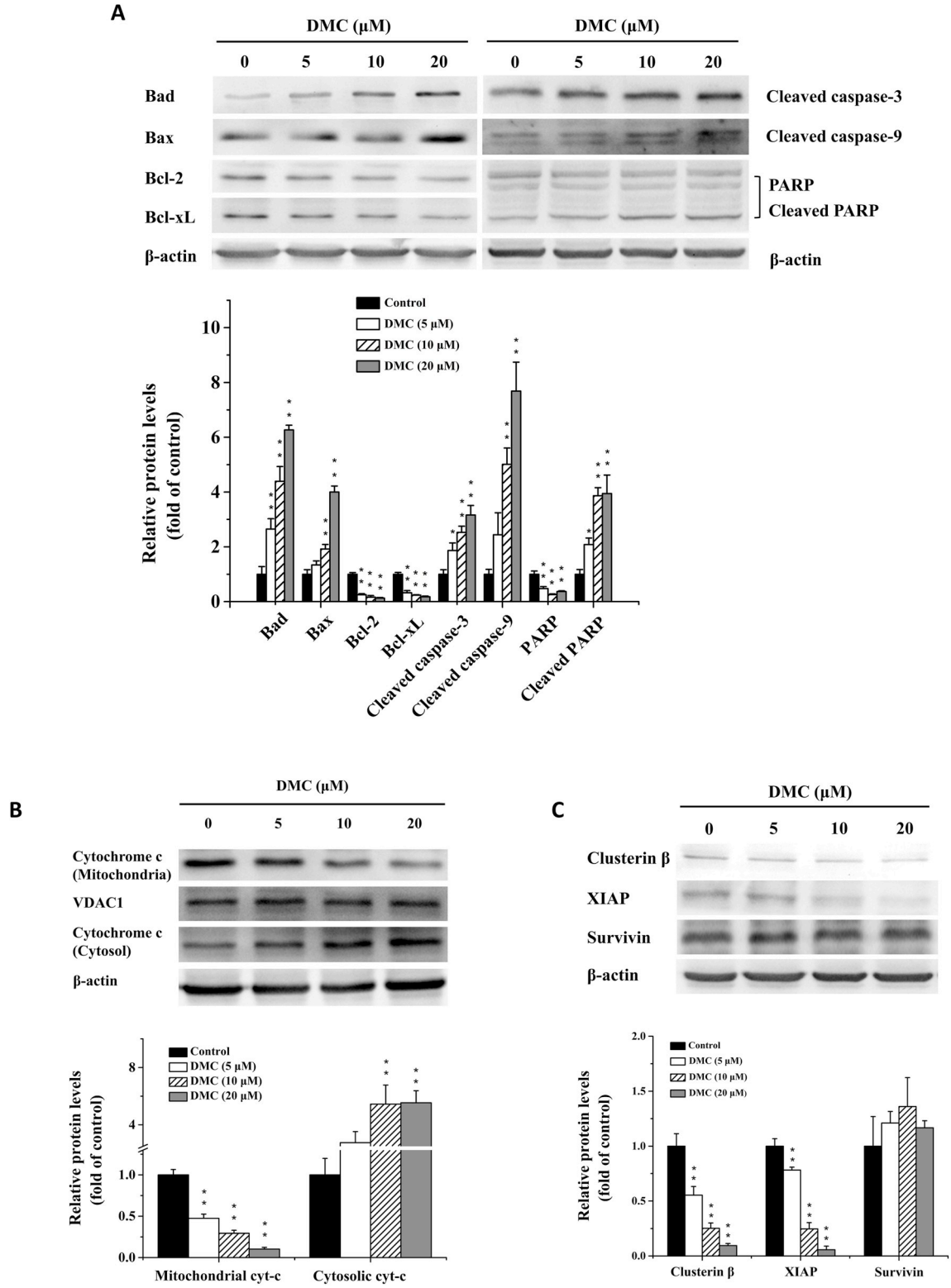

Fig. 5. DMC regulated the expression of key proteins in mitochondrial apoptosis pathway in BEL-7402/5-FU cells. After BEL-7402/5-FU cells were incubated with indicated concentrations of DMC for 24 h, the whole-cell lysates, cytosolic and mitochondrial fractions were prepared, and the expression levels of Bad, Bax, Bcl-2, Bcl-xL, cleaved caspase-3, cleaved caspase-9 and PARP/cleaved PARP (A), cytoplasmic and mitochondrial cytochrome c (B), clusterin β, XIAP and survivin (C) were determined by western blotting. β-actin served as the loading control for the total protein and the cytoplasmic protein, and VDAC1 served as the loading control for the mitochondrial protein. Data are presented as mean ± SD. Results are representative of three independent experiments. (*) $P < 0.05$ and (**) $P < 0.01$, compared with the control.

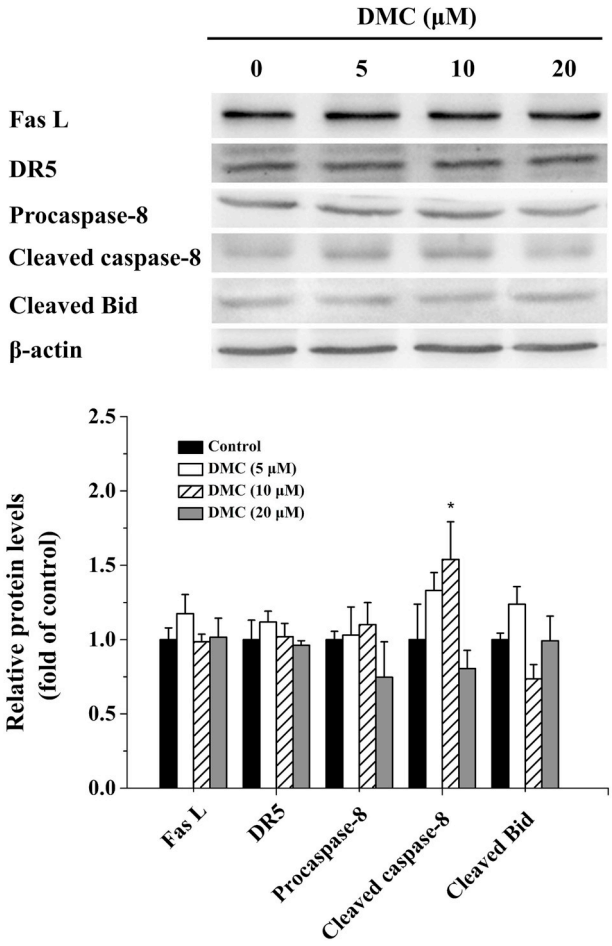

Fig. 6. Effect of DMC on extrinsic apoptotic pathway in BEL-7402/5-FU cells. After treatment with DMC for 24 h, the whole-cell lysates were prepared, and the expression levels of Fas L, DR5, procaspase-8, cleaved caspase-8 and cleaved Bid were determined by western blotting. β-actin served as the loading control. Data are presented as mean ± SD. Results are representative of three independent experiments. (*) $P < 0.05$ and (**) $P < 0.01$, compared with the control.

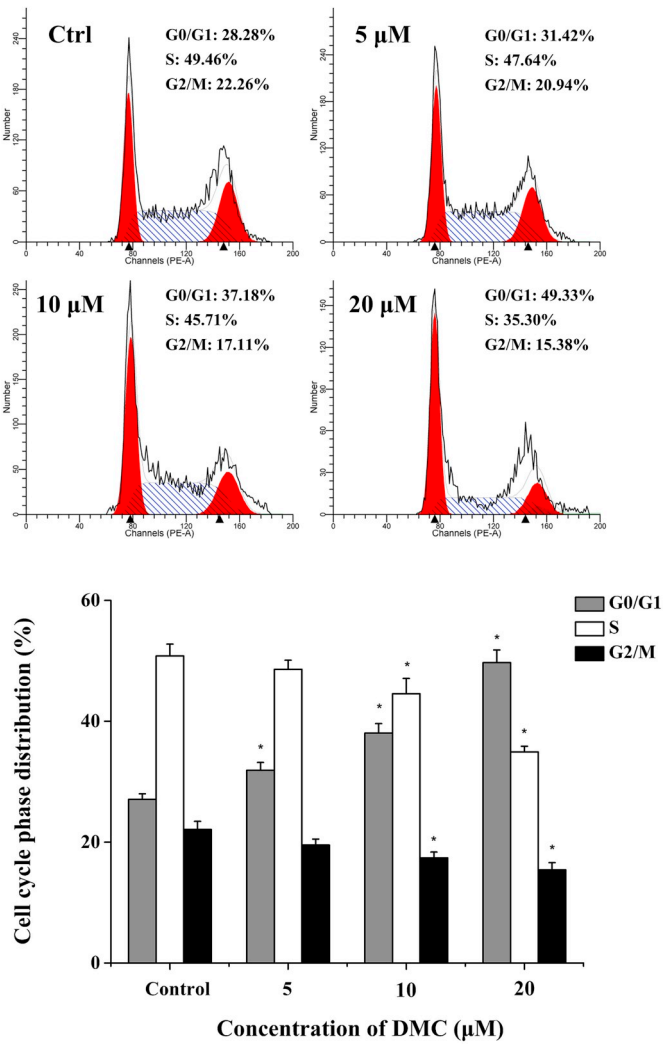

Fig. 7. DMC induced G1 cell cycle arrest in BEL-7402/5-FU cells. After incubation with DMC for 24 h, cells were fixed in 70% cold ethanol, followed by propidium iodide staining. Each sample was subjected to flow cytometry. Data are presented as mean ± SD. Results are representative of three independent experiments. (*) $P < 0.05$ and (**) $P < 0.01$, compared with the control.

inhibitory effect it brought. Furthermore, DMC blocked cell cycle progression at G1 phase, which was another mechanism for its tumor-inhibitory capacity.

Apoptosis is a genetically coded 'suicide' programme that plays pivotal roles in diverse physiologic and pathologic processes. It can be triggered through the mitochondrial (the intrinsic) pathway or the death receptor (the extrinsic) pathway depending on multifarious stimuli. The initiation of the intrinsic apoptotic pathway is mediated by the Bcl-2 family responding to internal stress, such as ER stress and DNA damage. Among the mediating factors, the ratio of Bcl-2/Bax is a crucial button for the induction of apoptosis since the raise of it leads to the formation of mitochondrial outer membrane pore. Once the pore is formed, mitochondrial cytochrome c will be released into the cytosol. The apoptosome assembled by cytoplasmic cytochrome c and Apaf-1 then cleaves procaspase-9 to initiate its active form, cleaved caspase-9, which sequentially activates caspase-3 and triggers a series of cell death reactions (Mohammad et al., 2015). The inhibitors of apoptosis proteins (IAPs) commonly function as suppressors of downstream pro-apoptotic factors such as caspase-3, -6, -7, -9. (Deveraux et al., 1998). Additionally, ROS has been reported to be involved in the intrinsic apoptotic pathway initiation since it can induce the mitochondrial permeability transition (PT) pore opening, thus releasing some apoptotic-inducing proteins into the cytoplasm and triggering the caspase cascade (Qi et al., 2019). The evasion of apoptosis is one of the main causes of chemoresistance in cancers (Yang et al., 2018). In this study, we found that Bcl-2 and Bcl-xL were downregulated by DMC and Bax and Bad were upregulated. Besides, cytochrome c was released from the mitochondria into the cytosol after DMC treatment. As a result, cleaved caspase-3 and -9 were remarkably increased. PARP, one of the substrates of caspase-3, was decreased, and cleaved PARP was increased. Recent studies have reported similar apoptotic mechanisms of flavonoid-mediated anti-tumor effects in cancer cells (Hsu et al., 2018; Kaushik et al., 2018). Apoptosis inhibitors like clusterin β and XIAP were observed to be attenuated, but no apparent alteration in survivin was observed. Moreover, an increased level of intracellular ROS was observed after DMC treatment. In addition, no significant alteration was observed in the levels of key proteins of the extrinsic pathway after DMC exposure. These results indicated that DMC induced apoptosis in

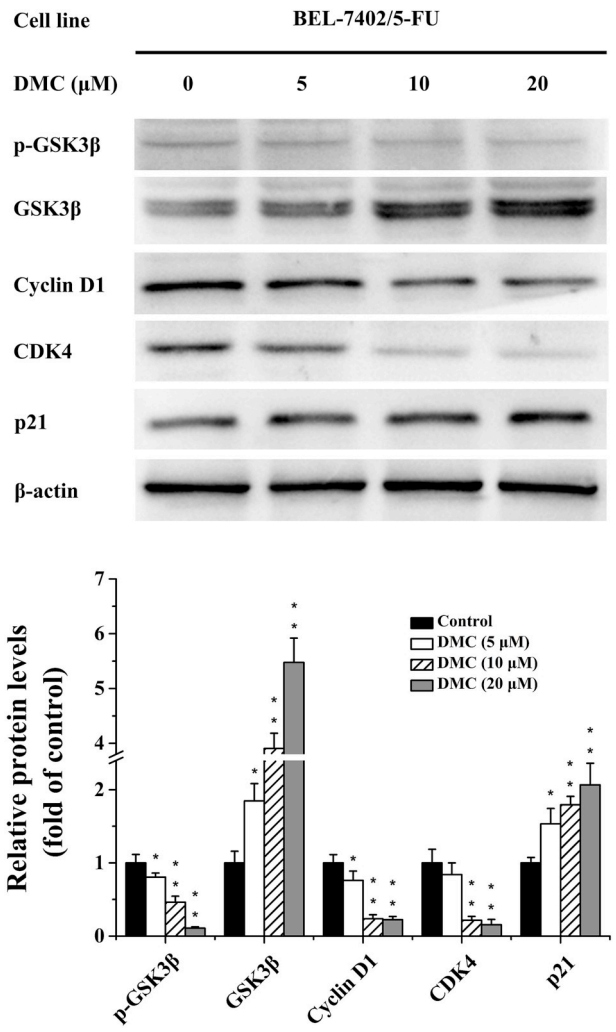

Fig. 8. DMC modulated the levels of key proteins related to G1 cell cycle in BEL-7402/5-FU cells. After treatment with indicated concentrations of DMC for 24 h, the whole-cell lysates were prepared, and the levels of p-GSK3β, GSK3β, cyclin D1, CDK4 and p21 were determined by western blotting. β-actin served as the loading control. Data are presented as mean ± SD. Results are representative of three independent experiments. (*) $P < 0.05$ and (**) $P < 0.01$, compared with the control.

BEL-7402/5-FU cells mainly through the mitochondria-mediated apoptotic pathway.

Cell cycle progression comprises a set of chronologically-specific activities responsible for DNA duplication and cell division. A complete cell cycle consists of four phases (G0/G1, S, G2 and M). The shift from G1 to S phase was triggered by the interaction of cyclin D1/CDK4 (Cicenas et al., 2014). Members of CKIs, such as p16, p21 and p27, negatively regulate cell cycle from G1 to S phase via inactivation of the cyclin D1/CDK4 complex. Besides, phosphorylation of cyclin D1 on Thr-286 by GSK3β promotes the proteasomal degradation of cyclin D1 (Vivanco and Sawyers, 2002). Cell cycle dysregulation is correlated with carcinogenesis. Therapeutics targeting cell cycle regulators have aroused considerable interest. Herein, we found that DMC induced cell cycle arrest at G1 phase and reduced the levels of p-GSK3β, cyclin D1 and CDK4. Moreover, GSK3β and p21, inhibitors of cyclin D1 and CDK4, were increased after DMC treatment. These results demonstrated that DMC impeded cell cycle progression at G1 phase through downregulation of p-GSK3β, cyclin D1 and CDK4 and upregulation of GSK3β and p21. Likewise, other studies reported that flavonoids can block G1 cell cycle phase in diverse types of tumor cells (Wang et al., 2018a,b; Zhou et al., 2017a,b).

As is well established, p53 is a pivotal tumor suppressor principally modulating the process of cell cycle blockage and apoptosis. Transcriptional activation of pro-apoptotic genes, such as PUMA, Noxa, Bax (Meek, 2004) and Bad (Jiang et al., 2007), by p53 is essential for mitochondrial apoptosis. Moreover, p53 also serves as a transcription suppressor of anti-apoptotic genes like Bcl-xL (Sugars et al., 2001). Likewise, NF-κB can target the anti-apoptotic genes like Bcl-2 and Bcl-xL, resulting in the suppression of apoptosis machinery. Therefore, it is reasonable for us to identify p53 and NF-κB as targets of DMC for the mitochondrial apoptosis induction in HCC. AKT, a serine/threonine kinase commonly activated in human cancers, is considered to be associated with apoptosis resistance and carcinogenesis (Hong et al., 2012). AKT activates Mdm2 through direct phosphorylation on Ser-166, thereby facilitating Mdm2 nuclear localization and the sequential degradation of p53 (Zhou et al., 2001). Meanwhile, NF-κB is activated through AKT direct phosphorylation on IKK and the consequent IκB-α degradation. With regard to cell cycle regulation, AKT positively modulates cyclin D1 level through inactivation of GSK3β. Specifically, the AKT-dependent phosphorylation of GSK3β on Ser-9 suppresses its kinase activity for Thr-286 of cyclin D1, which inhibits the nuclear export and the cytoplasmic proteasomal degradation of cyclin D1 (Shimura et al., 2012). Therapeutics targeting AKT signaling possess immense potential for inhibiting tumor multiplicity and overcoming chemoresistance (Mabuchi et al., 2015). In this study, the effects of DMC on p53, NF-κB, Mdm2, IKK and AKT were assessed. The western blotting results showed that both nuclear and cytoplasmic p53 were augmented after 2–8 h of DMC treatment. Consistently, a decrease in phosphorylation of AKT and Mdm2 was detected. The nuclear translocation of NF-κB inhibited by DMC was observed through Western blot analysis and was verified by immunofluorescence. In addition, IKK was found to be dephosphorylated after DMC treatment as well. In brief, Mdm2/p53 and IKK/NF-κB were modulated by DMC through the inhibition of AKT, which might be the molecular mechanism for DMC-mediated apoptosis and G1 phase arrest.

Moreover, we found that transfection with AKT-siRNA attenuated the reduction of Bcl-2 and the increase of Bax and Bad protein expression induced by DMC, denoting that AKT played a critical role in DMC-mediated apoptosis of BEL-7402/5-FU cells. In view of these results, DMC may be a potential natural agent for 5-FU-resistant HCC therapy.

5. Conclusions

In conclusion, this study demonstrated that DMC induced apoptosis in BEL-7402/5-FU cells through the mitochondria-dependent apoptotic pathway. Meanwhile, DMC induced G1 cell cycle arrest by down-regulating cyclin D1 and CDK4 and upregulating GSK3β and p21. Most importantly, the inactivation of PI3K/AKT induced by DMC further led to the suppression of Mdm2 and IKK, which ultimately resulted in an increase in p53 levels and an inhibition of NF-κB nuclear translocation. Collectively, DMC mediated apoptosis and arrest of G1 cell cycle phase through inhibiting PI3K/AKT signaling pathway. Taken together, DMC might be used as a potential natural therapeutic agent against HCC in the future.

Conflicts of interest

The authors declare no competing financial interest.

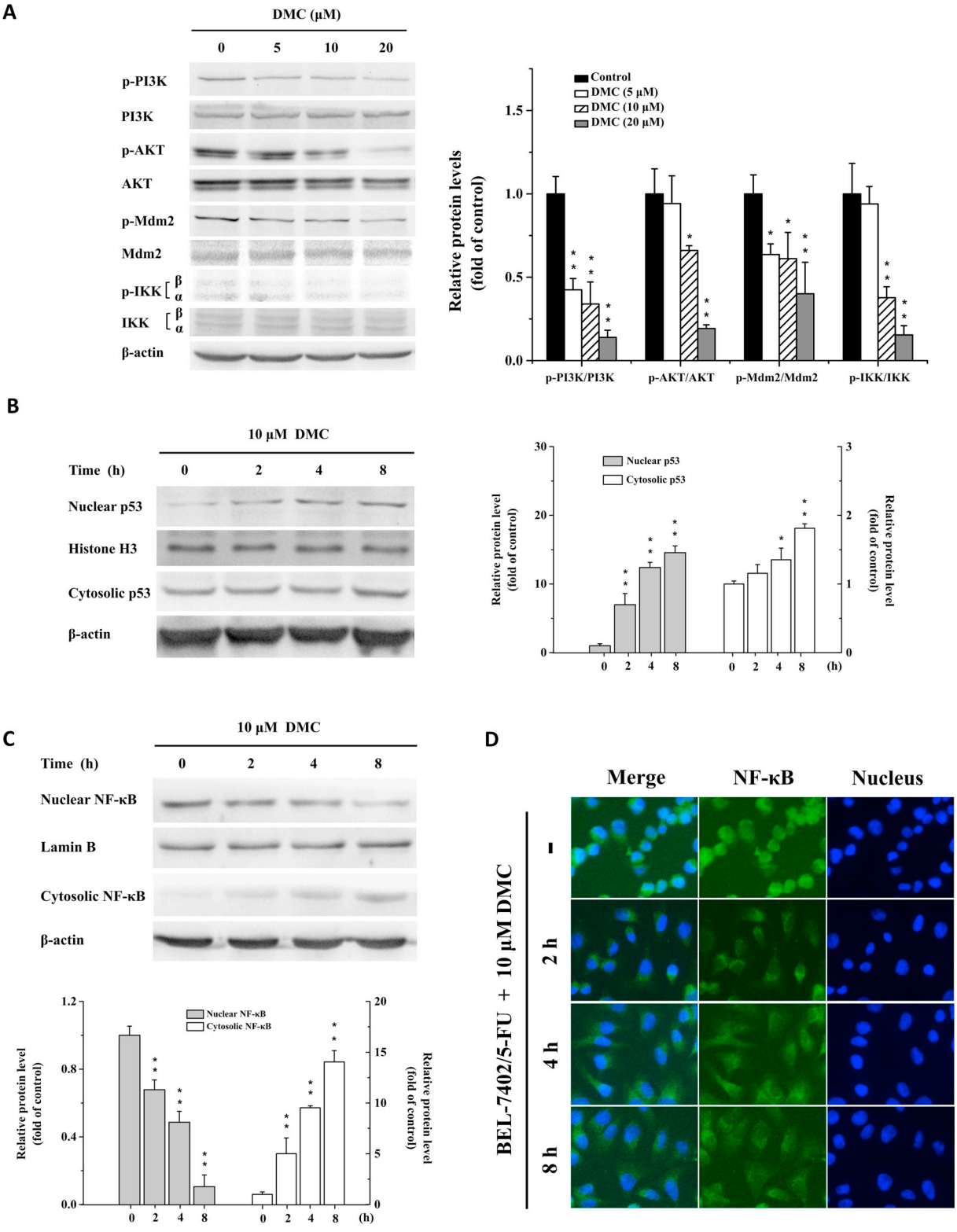

Fig. 9. DMC regulated key proteins of PI3K/AKT pathway in BEL-7402/5-FU cells.

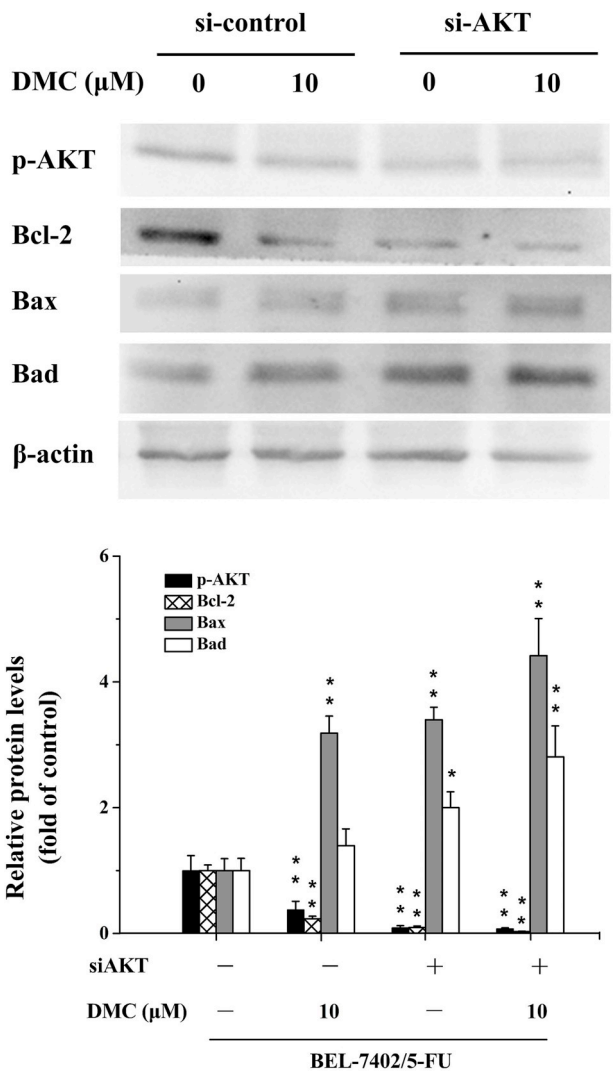

Fig. 10. DMC regulated the expression of apoptosis-related proteins through the suppression of AKT. BEL-7402/5-FU cells were transfected with non-targeting control siRNA or AKT-siRNA for 5 h prior to treatment with 10 μM DMC for an additional 48 h. Levels of p-AKT, Bcl-2, Bax and Bad were determined by western blotting. Data are presented as mean ± SD. Results are representative of three independent experiments. (*) $P < 0.05$ and (**) $P < 0.01$, compared with the control.

Declaration of interests

The authors declare that they have no known competing financial interests or personal relationships that could have appeared to influence the work reported in this paper.

The authors declare the following financial interests/personal relationships which may be considered as potential competing interests:

Acknowledgements

This work was supported by the National Natural Science Foundation of China (No. 31600273), the General Financial Grant from the China Postdoctoral Science Foundation (2016M601532, 2018T110359), as well as by the Opening Project of Zhejiang Provincial Preponderant and Characteristic Subject of Key University (Traditional Chinese Pharmacology), Zhejiang Chinese Medical University (ZYAOX2018022).

Abbreviations

5-FU	5-fluorouracil
CCNs	cyclins
CDKs	cyclin-dependent kinases
CKIs	cyclin-dependent kinase inhibitors
Cyt-c	cytochrome c
DCFH-DA	2′,7′-dichlorofluorescein diacetate
DMC	2′,4′-Dihydroxy-6′-methoxy-3′,5′-dimethylchalcone
HCC	Hepatocellular carcinoma
IAPs	inhibitors of apoptosis proteins
IKK	inhibitor of NF-κB (IκB) kinase
Mdm2	Murine double minute 2
MTT	3-(4,5-dimethylthiazol-2-yl)-2,5-diphenyltetrazolium bromide
NF-κB	nuclear factor-kappa B
PI3K	phosphatidylinositol 3-kinase
siRNA	small interfering RNA
ROS	reactive oxygen species
SD	standard deviation

Appendix A. Supplementary data

Supplementary data to this article can be found online at https://doi.org/10.1016/j.fct.2019.05.041.

References

Asghar, U., Witkiewicz, A.K., Turner, N.C., Knudsen, E.S., 2015. The history and future of targeting cyclin-dependent kinases in cancer therapy. Nat. Rev. Drug Discov. 14, 130–146.

Bonelli, P., Tuccillo, F.M., Borrelli, A., Schiattarella, A., Buonaguro, F.M., 2014. CDK/CCN and CDKI alterations for cancer prognosis and therapeutic predictivity. BioMed Res. Int. 2014, 361020.

Cicenas, J., Kalyan, K., Sorokinas, A., Jatulyte, A., Valiunas, D., Kaupinis, A., Valius, M., 2014. Highlights of the latest advances in research on CDK inhibitors. Cancers 6, 2224–2242.

Deveraux, Q.L., Roy, N., Stennicke, H.R., Arsdale, T.V., Zhou, Q., Srinivasula, S.M., Alnemri, E.S., Salvesen, G.S., Reed, J.C., 1998. IAPs block apoptotic events induced by caspase-8 and cytochrome c by direct inhibition of distinct caspases. EMBO J. 17, 2215–2223.

Ferlay, J., Soerjomataram, I., Dikshit, R., Eser, S., Mathers, C., Rebelo, M., Parkin, D.M., Forman, D., Bray, F., 2015. Cancer incidence and mortality worldwide: sources, methods and major patterns in GLOBOCAN 2012. Int. J. Cancer 136, E359–E386.

Gu, W., Fang, F.F., Li, B., Cheng, B.B., Ling, C.Q., 2012. Characterization and resistance mechanisms of a 5-fluorouracil-resistant hepatocellular carcinoma cell line. Asian Pac. J. Cancer Prev. APJCP 13, 4807–4814.

He, J.F., Ge, M.H., Zhu, X., Chen, C., Tan, Z., Li, Y.N., Gu, Z.Y., 2008. Expression of RUNX3 in salivary adenoid cystic carcinoma: implications for tumor progression and prognosis. Cancer Sci. 99, 1334–1340.

Hong, S.W., Jung, K.H., Lee, H.S., Choi, M.J., Son, M.K., Zheng, H.M., Hong, S.S., 2012. SB365 inhibits angiogenesis and induces apoptosis of hepatocellular carcinoma through modulation of PI3K/Akt/mTOR signaling pathway. Cancer Sci. 103, 1929–1937.

Hou, Y.Q., Yao, Y., Bao, Y.L., Song, Z.B., Yang, C., Gao, X.L., Zhang, W.J., Sun, L.G., Yu, C.L., Huang, Y.X., Wang, G.N., Li, Y.X., 2016. Juglanthraquinone C induces intracellular ROS increase and apoptosis by activating the Akt/Foxo signal pathway in HCC cells. Oxid. Med. Cell. Longev. 2016, 4941623.

Hsu, Y.N., Shyu, H.W., Hu, T.W., Yeh, J.P., Lin, Y.W., Lee, L.Y., Yeh, Y.T., Dai, H.Y., Perng, D.S., Su, S.H., Huang, Y.H., Su, S.J., 2018. Anti-proliferative activity of biochanin A in human osteosarcoma cells via mitochondrial-involved apoptosis. Food Chem. Toxicol. 112, 194–204.

Huang, H.Y., Niu, J.L., Lu, Y.H., 2012. Multidrug resistance reversal effect of DMC derived from buds of *Cleistocalyx operculatus* in human hepatocellular tumor xenograft model. J. Sci. Food Agric. 92, 135–140.

Huang, H.Y., Niu, J.L., Zhao, L.M., Lu, Y.H., 2011. Reversal effect of 2',4'-dihydroxy-6'-methoxy-3',5'-dimethylchalcone on multi-drug resistance in resistant human hepatocellular carcinoma cell line BEL-7402/5-FU. Phytomedicine 18, 1086–1092.

Jeong, J.H., An, J.Y., Kwon, Y.T., Rhee, J.G., Lee, Y.J., 2009. Effects of low dose quercetin: cancer cell-specific inhibition of cell cycle progression. J. Cell. Biochem. 106, 73–82.

Jiang, P., Du, W.J., Wu, M., 2007. p53 and Bad: remote strangers become close friends. Cell Res. 17, 283–285.

Kaushik, S., Shyam, H., Sharma, R., Balapure, A.K., 2018. Dietary isoflavone daidzein synergizes centchroman action via induction of apoptosis and inhibition of PI3K/Akt pathway in MCF-7/MDA MB-231 human breast cancer cells. Phytomedicine 40, 116–124.

Lewis-Wambi, J.S., Jordan, V.C., 2009. Estrogen regulation of apoptosis: how can one hormone stimulate and inhibit? Breast Cancer Res. 11, 206.
Mabuchi, S., Kuroda, H., Takahashi, R., Sasano, T., 2015. The PI3K/AKT/mTOR pathway as a therapeutic target in ovarian cancer. Gynecol. Oncol. 137, 173–179.
Meek, D.W., 2004. The p53 response to DNA damage. DNA Repair 3, 1049–1056.
Mohammad, R.M., Muqbil, I., Lowe, L., Yedjou, C., Hsu, H.Y., Lin, L.T., Siegelin, M.D., Fimognari, C., Kumar, N.B., Dou, Q.P., Yang, H.J., Samadi, A.K., Russo, G.L., Spagnuolo, C., Ray, S.K., Chakrabarti, M., Morre, J.D., Coley, H.M., Honoki, K., Fujii, H., Georgakilas, A.G., Amedei, A., Niccolai, E., Amin, A., Ashraf, S.S., Helferich, W.G., Yang, X.J., Boosani, C.S., Guha, G., Bhakta, D., Ciriolo, M.R., Aquilano, K., Chen, S., Mohammed, S.I., Keith, W.N., Bilsland, A., Halicka, D., Nowsheen, S., Azmi, A.S., 2015. Broad targeting of resistance to apoptosis in cancer. Semin. Canc. Biol. 35, S78–S103.
Momand, J., Jung, D., Wilczynski, S., Niland, J., 1998. The MDM2 gene amplification database. Nucleic Acids Res. 26, 3453–3459.
Nag, S., Zhang, X., Srivenugopal, K.S., Wang, M.H., Wang, W., Zhang, R., 2014. Targeting MDM2-p53 interaction for cancer therapy: are we there yet? Curr. Med. Chem. 21, 553–574.
Qi, S.S., Guo, L.Y., Yan, S.Z., Lee, R.J., Yu, S.Q., Chen, S.L., 2019. Hypocrellin A-based photodynamic action induces apoptosis in A549 cells through ROS-mediated mitochondrial signaling pathway. Acta Pharm. Sin. B 9, 279–293.
Saha, S., Bhattacharjee, P., Guha, D., Kajal, K., Khan, P., Chakraborty, S., Mukherjee, S., Paul, S., Manchanda, R., Khurana, A., Nayak, D., Chakrabarty, R., Sa, G., Das, T., 2015. Sulphur alters NFκB-p300 cross-talk in favour of p53-p300 to induce apoptosis in non-small cell lung carcinoma. Int. J. Oncol. 47, 573–582.
Shimura, T., Noma, N., Oikawa, T., Ochiai, Y., Kakuda, S., Kuwahara, Y., Takai, Y., Takahashi, A., Fukumoto, M., 2012. Activation of the AKT/cyclin D1/Cdk4 survival signaling pathway in radioresistant cancer stem cells. Oncogenesis 1, e12.
Sugars, K.L., Budhram-Mahadeo, V., Packham, G., Latchman, D.S., 2001. A minimal Bcl-x promoter is activated by Brn-3a and repressed by p53. Nucleic Acids Res. 29, 4530–4540.
Tao, J.Y., Jiang, L.L., Chen, X., 2018. Roles of microRNA in liver cancer. Liver Res 2, 61–72.
Vivanco, I., Sawyers, C.L., 2002. The phosphatidylinositol 3-kinase-AKT pathway in human cancer. Nat. Rev. Canc. 2, 489–501.
Vousden, K.H., Prives, C., 2009. Blinded by the light: the growing complexity of p53. Cell 137, 413–431.
Wang, J., Li, X.M., Bai, Z., Chi, B.X., Wei, Y., Chen, X., 2018a. Curcumol induces cell cycle arrest in colon cancer cells via reactive oxygen species and Akt/GSK3β/cyclin D1 pathway. J. Ethnopharmacol. 210, 1–9.
Wang, J., Zhang, Y.S., Thakur, K., Hussain, S.S., Zhang, J.G., Xiao, G.R., Wei, Z.J., 2018b. Licochalcone A from licorice root, an inhibitor of human hepatoma cell growth via induction of cell apoptosis and cell cycle arrest. Food Chem. Toxicol. 120, 407–417.
Wei, X., Mo, X.J., An, F.L., Ji, X., Lu, Y.H., 2018. 2',4'-Dihydroxy-6'-methoxy-3',5'-dimethylchalcone, a potent Nrf2/ARE pathway inhibitor, reverses drug resistance by decreasing glutathione synthesis and drug efflux in BEL-7402/5-FU cells. Food Chem. Toxicol. 119, 252–259.
Yang, C.D., Hou, A.H., Yu, C.F., Dai, L.L., Wang, W., Zhang, K.L., Shao, H.M., Ma, J.H., Xu, W.J., 2018. Kanglaite reverses multidrug resistance of HCC by inducing apoptosis and cell cycle arrest via PI3K/AKT pathway. OncoTargets Ther. 11, 983–996.
Ye, C.L., Liu, J.W., Wei, D.Z., Lu, Y.H., Qian, F., 2004. In vitro anti-tumor activity of 2',4'-dihydroxy-6'-methoxy-3',5'-dimethylchalcone against six established human cancer cell lines. Pharmacol. Res. 50, 505–510.
Ye, C.L., Qian, F., Wei, D.Z., Lu, Y.H., Liu, J.W., 2005. Induction of apoptosis in K562 human leukemia cells by 2',4'-dihydroxy-6'-methoxy-3',5'-dimethylchalcone. Leuk. Res. 29, 887–892.
Zhou, B.H.P., Liao, Y., Xia, W.Y., Zou, Y.Y., Spohn, B., Hung, M.C., 2001. HER-2/neu induces p53 ubiquitination via Akt-mediated MDM2 phosphorylation. Nat. Cell Biol. 3, 973–982.
Zhang, N., Yin, Y., Xu, S.J., Chen, W.S., 2008. 5-Fluorouracil: mechanisms of resistance and reversal strategies. Molecules 13, 1551–1569.
Zhang, Y., Chen, S.G., Wei, C.Y., Rankin, G.O., Ye, X.Q., Chen, Y.C., 2018. Flavonoids from Chinese bayberry leaves induced apoptosis and G1 cell cycle arrest via Erk pathway in ovarian cancer cells. Eur. J. Med. Chem. 147, 218–226.
Zhou, M.J., Zhang, Q., Zhao, J.F., Liao, M.M., Wen, S.L., Yang, M.Y., 2017a. Phosphorylation of Bcl-2 plays an important role in glycochenodeoxycholate-induced survival and chemoresistance in HCC. Oncol. Rep. 38, 1742–1750.
Zhou, M.L., Shen, S.Y., Zhao, X., Gong, X.G., 2017b. Luteoloside induces G0/G1 arrest and pro-death autophagy through the ROS-mediated AKT/mTOR/p70S6K signalling pathway in human non-small cell lung cancer cell lines. Biochem. Biophys. Res. Commun. 494, 263–269.